A Robust and Adaptive Framework for Localization under Varying Sensor Modalities*

Shaunak D. Bopardikar†

United Technologies Research Center Inc., 2855 Telegraph Ave Suite 410 Berkeley CA 94705 USA

Shuo Zhang‡

United Technologies Research Center, 411 Silver Lane East Hartford CT 06118 USA

Alberto Speranzon§

United Technologies Research Center, 411 Silver Lane East Hartford CT 06118 USA

This paper proposes a modular estimation framework that enhances robustness and adaptability of legacy filters, such as the standard Extended or Unscented Kalman Filter (EKF/UKF), in the presence of *sudden* and *unknown* events such as sensor failures, unavailability, change of accuracy and out-of-sequence measurements. The framework comprises of three main outer modules *wrapped* around a core legacy filter: 1) *Measurement gating*, to detect large changes in covariance of sensors and reject their measurements until a new consistent covariance estimate is obtained; 2) *Covariance estimation*, to estimate the accuracy of each sensor at all times and; 3) *Out-of-sequence processing*, to perform optimal, in terms of minimum mean squared error, estimation when sensor measurements become out-of-sequence in time for any arbitrary arrival order.

We apply this framework to localize a real mobile vehicle moving in an unknown environment, equipped with various suites of sensors. The contributions of this paper are two-fold. First, we demonstrate a successful integration of the out-of-sequence processing algorithm with the other two modules around a standard EKF. Second, we show via numerical simulations, that under randomly generated events of sensor failure, accuracy changes, unavailability or delays, our proposed approach performs significantly better than a simple baseline EKF. We report the results applied to simulated scenarios, as well as on multiple real data sets.

I. Introduction

A. Motivation

Positioning systems, capable of working without the continuous presence of a Global Positioning System (GPS), are required for navigation in environments consisting of dense urban areas and man-made structures as well as indoor, underground and undersea. This type of technology is necessary for autonomous navigation, for providing more sophisticated position-based services, to enhance asset tracking for security and safety and to enable effective first-response operations in dangerous environments, just to mention a few.

The problem of positioning in GPS degraded/denied environment has been extensively researched in the last 40 years, strongly boosted by the development of the Kalman filter in the 60s, which provided an efficient implementation of estimators/filters. Although this area can be certainly considered very mature,

*The authors gratefully acknowledge support from DARPA, contract number FA8650-11-C-7139, and the United Technology Research Center. The views expressed are those of the author and do not reflect the official policy or position of the Department of Defense or the U.S. Government. Approved for Public Release, Distribution Unlimited.

†Senior Research Scientist. Email: bopardsd@utrc.utc.com

‡Senior Research Scientist. Email: zhangs1@utrc.utc.com

§Staff Research Scientist. Email: Email: sperana@utrc.utc.com

with compelling results available in the literature, solutions are often designed and demonstrated in particular environments, with particular lighting and weather conditions, either indoor or outdoor, etc. However, as applications increasingly rely on position information, the filtering and fusion process needs to be capable of working in any environmental condition, during the day or night, for many consecutive days without the need of re-calibrating or re-initializing the system.

This has brought a paradigm shift in the development of position and navigation technologies: from accuracy as the objective to solutions that need to be robust, easy to integrate and accurate. Therefore solutions not only need to provide an accurate position estimate, but they also need to work even if sensors change their behavior online in an unknown fashion. The uncertainty on these changes is typically caused by complex and unforeseeable changes in the environment. For example, a stereo camera with a landmark detection algorithm will provide the relative position of the landmark from the observer with very different accuracy when the cameras are pointing directly to the sun, or in fog.

In this paper, we propose a modular estimation framework that enables robust positioning and navigation under unknown varying sensor characteristics and availability. The proposed scheme can be "wrapped" around a standard navigation filter, such as EKF or UKF, thus enabling retrofit of existing solutions, and thus faster and cheaper integration. The limiting factor of considering EKF or UKF can be relaxed by building Particle Filters in which each of the particle implements the proposed robust and adaptive filter.

B. Related Work

One of the key research areas that deal with varying sensor characteristics during estimation is *Adaptive Kalman Filtering*. Seminal works[1] and[2] propose online techniques to determine the measurement and process noise covariance matrices. In the case of linear systems with Gaussian noise, these techniques rely on the whiteness property of the innovations sequence for the filter to be performing optimally. A self-tuning Kalman filter via stochastic approximations is presented in.[3] However, stochastic approximations tend to be slow to converge and require a good initial guess. More recently, heuristics based on sample averages have been proposed in literature such as.[4,5] These techniques have been demonstrated to work even on non-linear systems involving the Extended Kalman Filter (see[6,7]). In[8] and in,[9] the authors have presented a fuzzy neural network in conjunction with adaptive extended Kalman Filter to enhance the learning of the measurement noise covariance. In,[10] the authors demonstrate this technique on a low-cost INS/GPS system and show improvement in the navigation estimation accuracy. In,[11] the authors integrate a fuzzy version of the outlier detection technique used in this paper with adaptive measurement error covariance estimation and demonstrate results on experimental data from autonomous underwater vehicle trials.

Another key research area which is related to this work is *outlier rejection*. One of the most popular techniques in the area of estimation to detect and reject erroneous measurements is *gating*, known alternatively as the *chi-squared test*, described in.[12–14] This technique is widely used in performing data association, as shown in.[15,16] From the performance point-of-view,[17] derives a modified Riccati equation that approximately quantifies the dependence of the estimation error covariance on parameters such as gate thresholds and probability of false alarms. Given a set of measurements, false-alarm probability, and a signal-to-noise ratio, the celebrated Neyman Pearson detector has been known to minimize the false dismissal probability (cf.[18]). When the measurement is much weaker compared to the noise, locally optimum detectors have been proposed.[19]

In a centralized multisensor system, there are usually different time delays in transmitting measurements to a central processor. This can lead to situations where measurements from different sensors arrive out-of-sequence, see Figure 1. This is often referred as the out-of-sequence measurement (OOSM) problem. The OOSM problem was initially investigated in target tracking applications,[20] and thereafter many researchers have studied the OOSM problem in various areas, such as wireless sensor network,[21] robotics[22] and navigation.[23] In this paper, we opt for a most recent OOSM algorithm from,[24] which is the optimal one, in the minimum mean square sense, for multiple OOSMs with arbitrary delay and arriving order.

C. Contributions

The contributions of this paper are two-fold. First, we propose an integrated framework comprising of three main modules that can be easily wrapped around a legacy filter such as an Extended Kalman Filter, to make the estimation process robust to major disturbances in many operational environments, such as sudden or gradual changes in measurement error statistics of one or many sensors and random transmission delays.

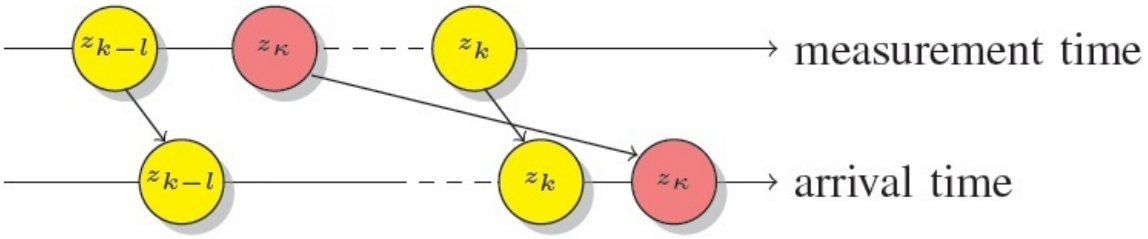

Figure 1. Example of out-of-sequence measurements. Measurements are generated at some *measurement time* but arrive at the filter at a later *arrival time*. Because of delays, events (such as on/off of sensors, etc.) the measurement produced at time κ is received after the measurement produced at time k.

This approach, illustrated in Figure 2, merges a gating block along with a residuals-based covariance learning scheme, to reject measurements being generated out of excessively large error covariances. The second block is a covariance update routine which continuously keeps a track of a sensor's accuracy (whenever the measurements are available) over time. The third block leverages the most recent advance in out-of-sequence measurement processing to achieve delay-tolerant navigation. We apply this general framework to a problem of localizing a mobile vehicle, equipped with different combinations of the following suite of sensors: Inertial Measurement Unit (IMU), Global Positioning System (GPS), Barometric Altimeter, Magnetic Compass, Odometer, Inclinometer, Time difference of Arrival sensor, and 2D Laser scanner. Specifically, we focus on scenarios in which the GPS is either intermittently available or completely unavailable.

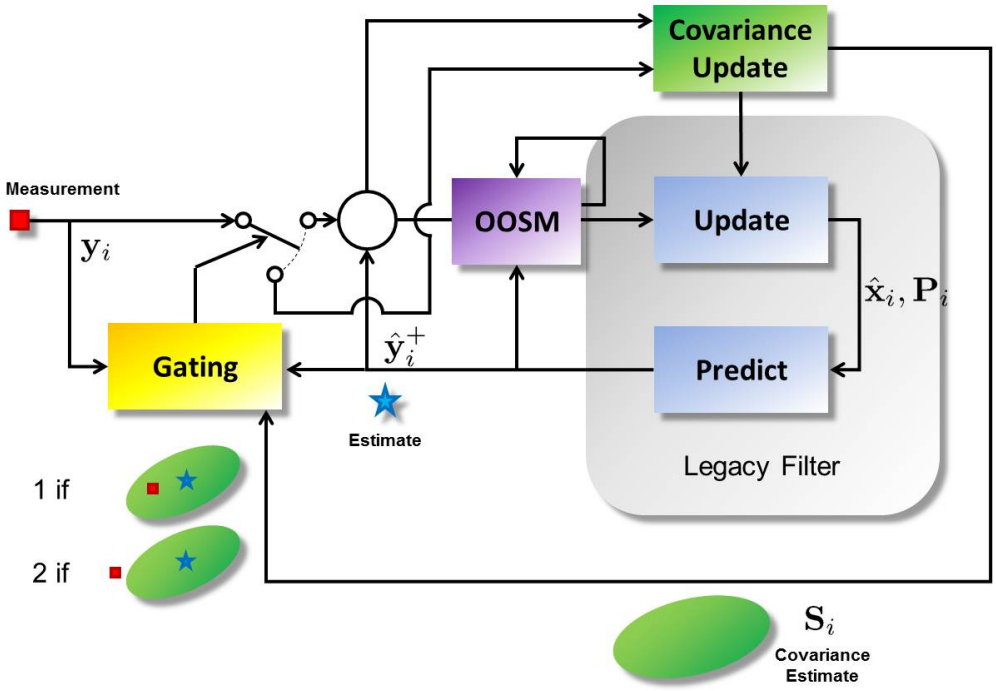

Figure 2. A skeleton of the proposed framework. The novelty lies in the integration of the gating and the covariance update blocks together with a legacy filter such as the EKF to make it robust and adaptive to changes in sensor accuracies.

Our second contribution is that we demonstrate, via extensive numerical simulations, that under randomly generated events of sensor failure/accuracy changes, our proposed approach outperforms significantly a standard/legacy baseline EKF. During a typical mission, we consider several stochastically generated *unknown events*, in which each sensor is either (i) functioning normally, or (ii) changes its accuracy, or (iii) is faulty, or (iv) is unavailable, or (v) reports measurements that may be out-of-sequence in time. We estab-

lish robustness as well as adaptability of our filtering scheme by reporting test results of our approach on simulated data sets as well as on real data sets. Another salient feature of our approach is that the filtering scheme uses the IMU to obtain the prediction at each time instant. Therefore, knowledge of the exact motion model of the vehicle is not necessary to obtain a good estimate of the vehicle's position and orientation.

D. Organization of this paper

This paper is organized as follows: Section II describes the problem formulation and the technical approach adopted. Section III describes the results of our approach on both simulated and real data sets. In particular, for the real data sets, we consider a scenario in which GPS is intermittent and a scenario which GPS is not available. Finally, the conclusions and future directions are discussed in Section IV.

II. Problem Set-up and Technical Approach

In this section, we present the mathematical model of the system and detail the technical approach.

A. The model

Consider the evolution of a dynamical system given by

$$\dot{\mathbf{x}}(t) = \mathbf{f}(\mathbf{x}(t), \mathbf{n}(t)),$$

where $\mathbf{x}(t) \in \mathbb{R}^{n_x}$ is the system state and $\mathbf{n}(t) \in \mathbb{R}^{n_n}$ is the process noise and $\mathbf{f}(.)$ is a vector field in $\mathbb{R}^{n_x}$ describing the dynamics of the system for time $t \in \mathbb{R}_{\geq 0}$. Let m be the number of sensors, and let the measurements from the sensors be generated as per the following equations:

$$\mathbf{y}_i(t) = \mathbf{h}_i(\mathbf{x}(t), \mathbf{v}_i(t)), \qquad \forall i \in \{1, \ldots, m\}, \tag{1}$$

where $\mathbf{v}_i(t) \in \mathbb{R}^{n_i}$ is the measurement noise, $\mathbf{h} : \mathbb{R}^{n_x} \times \mathbb{R}^{n_i} \to \mathbb{R}^{n_{y_i}}$ describes the i-th measurement equation. We assume that $\mathbf{n}(.), \mathbf{v}_i(.)$ are white Gaussian stochastic processes with zero-mean and mutually independent.

In our navigation problem, four references frames are used: WGS-84 frame, navigation frame, body frame and senor frame. The ENU coordinate (East-North-Up) is chosen as the navigation frame, the body frame is defined within our mobile vehicle platform and each sensor mounted on the platform has a unique sensor frame defined with respect to the body frame. We use a standard six-degrees-of-freedom (6DOF) model by assuming rigid movement of the vehicle. To mitigate IMU sensor drift, we also include the components of accelerator and gyroscope biases in the state. The resulting 16 dimensional state vector of our system is

$$\mathbf{x} = \begin{bmatrix} {}^N\mathbf{p}_B^T & {}^N\mathbf{v}_B^T & {}^B\mathbf{q}_N^T & \mathbf{b}_a^T & \mathbf{b}_g^T \end{bmatrix}^T,$$

where ${}^N\mathbf{p}_B = [x, y, z]^T$ and ${}^N\mathbf{v}_B = [v_x, v_y, v_z]^T$ represent the position and velocity vector of the vehicle in the navigation frame, ${}^B\mathbf{q}_N = [q_1, q_2, q_3, q_4]^T$ is the attitude quaternion presenting the rotation from the navigation frame to the body frame, $\mathbf{b}_a = [b_x^a, b_y^a, b_z^a]^T$ and $\mathbf{b}_g^T = [b_x^g, b_t^g, b_z^g]^T$ denote the accelerometer bias and gyroscope bias, respectively.

The continuous time dynamic equations with velocity and quaternion components driven by IMU measurements are

$$\begin{aligned}
{}^N\dot{\mathbf{p}}_B(t) &= {}^N\mathbf{v}_B(t), \\
{}^N\dot{\mathbf{v}}_B(t) &= \mathbf{C}({}^B\mathbf{q}_N(t))^T(\mathbf{a}_m(t) - \mathbf{b}_a(t) - \mathbf{n}_a(t)) - {}^N\mathbf{g}, \\
{}^B\dot{\mathbf{q}}_N(t) &= -\frac{1}{2}\mathbf{\Omega}(\boldsymbol{\omega}_m(t) - \mathbf{b}_g(t) - \mathbf{n}_g(t)){}^B\mathbf{q}_N(t), \\
\dot{\mathbf{b}}_a(t) &= \mathbf{M}_a\mathbf{b}_a(t) + \mathbf{n}_{\mathbf{b}_a}(t), \\
\dot{\mathbf{b}}_g(t) &= \mathbf{M}_g\mathbf{b}_g(t) + \mathbf{n}_{\mathbf{b}_g}(t),
\end{aligned}$$

where $\mathbf{a}_m$ and $\boldsymbol{\omega}_m$ are the respective accelerometer and gyroscope measurements, $\mathbf{n}_a$ and $\mathbf{n}_g$ are the corresponding white Gaussian noises (WGN), $\mathbf{C}({}^B\mathbf{q}_N)$ is the direction cosine matrix (DCM) and $\mathbf{\Omega}(\boldsymbol{\omega})$ is the skew-symmetric matrix[25] and ${}^N\mathbf{g}$ is the gravitational acceleration in the navigation frame. The IMU biases are modeled as first-order Gaussian-Markov processes driven by WGN $\mathbf{n}_{\mathbf{b}_a}$ and $\mathbf{n}_{\mathbf{b}_g}$. The IMU scale factor error (SFE), while not included in the state, is accounted for by using covariance inflation technique.[26]

B. Technical Approach: Robust and Adaptive Filtering

Out of the legacy filters, we adopt the EKF considering its excellent balance between complexity and performance. To achieve robust and adaptive filtering, our navigation solution is constructed in such a way to capture major disturbances in real world operational environments including outliers, transmission delays and sudden or slow changing sensors' accuracy, as well as numerical issues which cannot be ignored in practice. The detailed algorithm is described in Algorithm 1. We clearly consider the discrete-time version of the EKF as this is implemented on a computer.

Algorithm 1 Robust Adaptive EKF

if A received measurement is OOSM **then**
See Algorithm 2.
else
1) *Predict using IMU measurements:*

$$\hat{\mathbf{x}}(k|k-1) = \mathbf{f}_D(\hat{\mathbf{x}}(k-1|k-1), \mathbf{0})$$
$$\mathbf{P}(k|k-1) = \mathbf{F}(k-1)\mathbf{P}(k-1)\mathbf{F}(k-1)^T + \mathbf{Q}(k-1)$$

2) *Measurement gating:*
Let

$$\nu_i(k) = \mathbf{y}_i(k) - \mathbf{h}_i(\hat{\mathbf{x}}(k|k-1), \mathbf{0})$$
$$d = \sqrt{\nu_i(k)'(\mathbf{H}_i(k)\mathbf{P}(k|k-1)\mathbf{H}_i'(k) + \mathbf{R}_i(k))^{-1}\nu_i(k)}$$

Then

$$\gamma_{i,k} = \begin{cases} 1 & \text{if } d \leq \beta\,, \\ 0 & \text{otherwise} \end{cases}$$

3) *Update:*

$$\mathbf{K}_i(k) = \mathbf{P}(k|k-1)\mathbf{H}_i(k)' \cdot (\mathbf{H}_i(k)\mathbf{P}(k|k-1)\mathbf{H}_i'(k) + \hat{\mathbf{R}}_i(k))^{-1}$$
$$\hat{\mathbf{x}}(k) = \hat{\mathbf{x}}(k|k-1) + \gamma_{i,k}\mathbf{K}_i(k) \cdot (\mathbf{y}_i(k) - \mathbf{h}_i(\hat{\mathbf{x}}(k|k-1), \mathbf{0}))$$
$$\mathbf{P}(k|k) = (\mathbf{I} - \gamma_{i,k}\mathbf{K}_i(k)\mathbf{H}_i(k))\mathbf{P}(k|k-1) \cdot (\mathbf{I} - \gamma_{i,k}\mathbf{K}_i(k) \cdot \mathbf{H}_i(k))' + \gamma_{i,k}\mathbf{K}_i(k)\hat{\mathbf{R}}_i(k)\mathbf{K}_i(k)'$$

end if
4) *Estimate sensor accuracy:*
Let $r_i(k) = \mathbf{y}_i(k) - \mathbf{h}_i(\hat{\mathbf{x}}(k|k), \mathbf{0})$

$$\hat{\mathbf{R}}_i(k) = \begin{cases} \mathbf{R}_{i,nom} & \text{if } k \leq w_i \\ 1/w_i \sum_{t=k-w_i+1}^{k} r_i(t)r_i(t)' + & \\ \quad \mathbf{H}_i(k)\mathbf{P}(k|k)\mathbf{H}_i'(k) & \text{otherwise} \end{cases}$$

1. Prediction

The EKF state prediction is obtained using the IMU measurements and is given by

$$\hat{\mathbf{x}}(k+1|k) = \mathbf{f}_D(\hat{\mathbf{x}}(k|k), \mathbf{0}),$$

since the noises have zero mean, where $\mathbf{f}_D$ is the discretization of $\mathbf{f}$. The predicted covariance is

$$\mathbf{P}(k+1|k) = \mathbf{F}(k)\mathbf{P}(k|k)\mathbf{F}(k)^T + \mathbf{Q}(k),$$

where $\mathbf{F}(k)$ is the Jacobian of $\mathbf{f}_D(\mathbf{x}(k), \mathbf{n}(k))$ evaluated at $(\hat{\mathbf{x}}(k|k), \mathbf{0})$, and $\mathbf{Q}(k)$ is the process noise covariance.

2. Measurement Gating

To reject outliers and spurious measurements, measurement gating is used to validate the received measurements. We employ the Mahalanobis distance as the distance measure, which has been shown to be highly efficient and robust in various applications.[14] Specifically, at a time instant k, one has the predicted value of the measurement $\mathbf{h}_i(\hat{\mathbf{x}}(k|k-1))$, the covariance of which equals $\mathbf{H}(k)\mathbf{P}(k|k-1)\mathbf{H}'(k)+\mathbf{R}_i(k)$, where $\mathbf{H}_i(k)$ is the linearization of the measurement function $\mathbf{h}_i$ around $(\hat{\mathbf{x}}(k),\mathbf{0})$ and $\mathbf{R}_i(k)$ is the measurement error covariance at time k. Then, the true measurement $\mathbf{y}_i(k)$ will be in the following region

$$\mathcal{V}_k = \{\mathbf{y}_i : (\mathbf{y}_i - \mathbf{h}_i(\hat{\mathbf{x}}(k|k-1)))'(\mathbf{H}_i(k)\mathbf{P}(k|k-1)\mathbf{H}_i'(k) + \mathbf{R}_i(k))^{-1}(\mathbf{y}_i - \mathbf{h}_i(\hat{\mathbf{x}}(k|k-1))) \leq \beta^2\} \quad (2)$$

with a probability determined by the gate threshold β. For a given value of this probability, the threshold β can be calculated analytically.[14] A measurement is valid if lying in the region defined by (2), otherwise it is rejected.

3. Update

If a measurement passes the gate, then it is used to update the state. Instead of using the standard covariance update in KF, which can cause loss of symmetry due to numerical errors, we opt for the Joseph form[14] for the covariance update. The symmetry nature of the Joseph form makes it numerically much more stable than the standard update form.

4. Covariance Estimation

The fourth step consists of performing online covariance estimation to account for the changes in sensor accuracy. To estimate $\mathbf{R}_i(k)$ one candidate approach would be to subtract sample covariance of innovation $\nu_i(k)$ by $\mathbf{H}(k)\mathbf{P}(k|k-1)\mathbf{H}'(k)$ (which represents part of the uncertainty in the innovations due to system dynamics), namely,

$$\hat{\mathbf{R}}_i(k) = \frac{1}{w_i}\sum_{t=k-w_i+1}^{k} \nu_i(k)\nu_i(k)' - \mathbf{H}(k)\mathbf{P}(k|k-1)\mathbf{H}(k)' \quad (3)$$

However, because of the minus sign in (3), $\hat{\mathbf{R}}_i(k)$ can become negative definite and hence this approach is numerically unstable in practice.

We adopted the method from [7] as shown in Algorithm 1, step 4, which guarantees the estimated covariance is non-negative definite. This approach is based on the following theorem.

Theorem 1. *Let $r(k)$ denote the residual of a linear dynamical system, i.e.,*

$$r(k) = \mathbf{y}(k) - \hat{\mathbf{y}}(k|k) \quad (4)$$

where the subscript of sensor index has been omitted for simplicity of notation. Then the measurement noise covariance $\mathbf{R}(k)$ is given by

$$\mathbf{R}(k) = E\{r(k)r(k)'\} + \mathbf{H}(k)\mathbf{P}(k|k)\mathbf{H}(k)' \quad (5)$$

where operator E represents the expectation, and $\mathbf{H}(k)$ and $\mathbf{P}(k|k)\mathbf{H}(k)$ represent the measurement matrix and the updated state covariance, respectively.

A proof of Theorem 1 is given in Appendix A. By comparing with (3), one can see that the innovation $\nu(k)$ has been replaced by the residual $r(k)$ and the the predicted covariance $\mathbf{P}(k|k-1)$ has been replaced by the updated covariance $\mathbf{P}(k|k)$.

5. Out-of-Sequence Measurements

In certain applications various sensor measurements are available at different rates and at non-uniform intervals, arriving at the filter with stochastic time delays, etc. In order to deal with this there is the need to augment the proposed approach with an extra step that can take care of such situations. We described it below.

This step comprises of optimal out-of-sequence measurement updates. The standard Bayesian update for a regular in-sequence measurement ($\mathbf{y}_k$) is given by

$$p(\mathbf{x}_k|\mathbf{y}_{1:k}) \propto p(\mathbf{y}_k|\mathbf{x}_k)p(\mathbf{x}_k|\mathbf{y}_{1:k-1})$$

and it is well known that the optimal implementation of this standard Bayesian update is the Kalman filer under linear Gaussian (LG) assumption. The Bayesian update with an OOSM ($\mathbf{y}_\kappa$) can be written as

$$p(\mathbf{x}_k|\mathbf{y}_{1:k}, \mathbf{y}_\kappa) \propto \underbrace{p(\mathbf{x}_k|\mathbf{y}_{1:k})}_{\text{known}} \underbrace{p(\mathbf{y}_\kappa|\mathbf{x}_k, \mathbf{y}_{1:k-1})}_{\text{unknown}}$$

Hence the key is to obtain the unknown likelihood $p(\mathbf{y}_\kappa|\mathbf{x}_k, \mathbf{y}_{1:k-1})$, which fortunately can be obtained exactly.[27] Under the LG assumption, the optimal implementation of this OOSM Bayesian update can be found in[24] using the complete in-sequence information (CISI) framework. The proposed methodology is summarized in Algorithm 2. Note that the standard covariance update has to be used here as the Joseph form does not hold for an OOSM.

III. Results on Simulated and on Real Data Sets

In this section, we present the results of our proposed approach on a simulated as well as on two real data sets.

A. Simulated Scenario

For the simulations, we consider a mobile vehicle which obeys the following *Dubins*-like kinematics:[28]

$$\begin{aligned} \dot{x} &= \cos\theta\,, \qquad \dot{z} = u_z\,, \\ \dot{y} &= \sin\theta\,, \qquad \dot{\theta} = u_\theta\,, \end{aligned}$$

where the controls $u_z, u_\theta \in [-1, 1]$. The values of these two controls were pre-chosen as a function of time. Next, we generated the measurements for each of the sensors using the *ground truth*, i.e., the true positions and orientations of the vehicle. E.g., using three consecutive positions, one can determine the acceleration. Measurements were corrupted with noise of known statistics, but unknown to the estimation.

Five types of *events* were generated randomly during the course of the simulation and they were unknown to the filter. The first type was that a sensor functions normally, the second in which a sensor is unavailable, the third in which the sensor changed its accuracy, the fourth in which the sensor was faulty, and the fifth in which the sensor's measurements were out of sequence in time. The accuracy change corresponded to an increase in the sensor's measurement noise covariance by a factor of 5, while the fault corresponded to a factor of 10000.

Initial estimate for the filter was chosen randomly from a neighborhood around the ground truth. Initial nominal covariances were selected in the vicinity of the true values, and the moving average windows w_i were chosen such that they were close to half the number of sensor measurements in the duration of one event. The result of Algorithm 1 and Algorithm 2 for one realization of the events is shown in Figure 3. The plot also shows the corresponding root mean square error (RMSE) in the position with respect to the ground truth, along with the different events and their temporal generation. Figure 4 shows a plot of the RMSE averaged over 50 realizations of the events, generated in a Monte Carlo fashion. A video uploaded along with this paper shows a simulation with additional set of sensors. In this video, the true and the actual measurement values have been plotted for each sensor. The true vehicle position is shown in red, the estimated position in green and the gray trajectory is the ground truth.

B. Results on Real Scenario

In this section, we report the results of our approach on data sets obtained from two different real scenarios. The first scenario is that of a mobile vehicle that has access to GPS, while in the second scenario, GPS signal is unavailable. In both cases, events related to sensors' characteristics are generated stochastically, similar to Section A.

Algorithm 2 CISI OOSM Processing

Assume $t_{k-l} \leq t_\kappa < t_{k-l+1}$ for a l-lag OOSM.

Step 1: Predict using IMU measurements:

$$\hat{\mathbf{x}}(\kappa|k-l) = \mathbf{f}_D(\hat{\mathbf{x}}(k-l|k-l), \mathbf{0})$$
$$\mathbf{P}(\kappa|k-l) = \mathbf{F}(k-l)\mathbf{P}(k-l)\mathbf{F}(k-l)^T + \mathbf{Q}(k-l)$$

Step 2: Update $\hat{\mathbf{x}}(\kappa|\kappa)$ using OOSM $\mathbf{y}_i(\kappa)$.

Step 3: Update all the states after t_κ up to current time t_k using OOSM $\mathbf{y}_i(\kappa)$.

for $j = k-l+1 : k$ **do**

1) *Obtain smoothed state and covariance at time t_κ, as well as crosscovariance between t_κ and t_j.*

$$\hat{\mathbf{x}}(\kappa|j) = \hat{\mathbf{x}}(\kappa|j-1) + \mathbf{P}(j-1,\kappa|j-1)'\mathbf{F}(j,j-1)' \cdot \mathbf{P}(j|j-1)^{-1}\left[\hat{\mathbf{x}}(j|j) - \hat{\mathbf{x}}(j|j-1)\right]$$
$$\mathbf{P}(\kappa|j) = \mathbf{P}(\kappa|j-1) - \mathbf{P}(j-1,\kappa|j-1)'\mathbf{F}(j,j-1)' \cdot \mathbf{P}(j|j-1)^{-1}[\mathbf{P}(j|j-1) - \mathbf{P}(j|j)]\cdot$$
$$\mathbf{P}(j|j-1)^{-1}\mathbf{F}(j,j-1)\mathbf{P}(j-1,\kappa|j-1)$$
$$\mathbf{P}(j,\kappa|j) = \mathbf{P}(j|j)\mathbf{P}(j|j-1)^{-1}\mathbf{F}(j,j-1) \cdot \mathbf{P}(j-1,\kappa|j-1)$$

2) *OOSM gating:*
Let

$$\nu_i(\kappa) = \mathbf{y}_i(\kappa) - \mathbf{h}_i(\hat{\mathbf{x}}(\kappa|j), \mathbf{0})$$
$$d = \sqrt{\nu_i(\kappa)'(\mathbf{H}_i(\kappa)\mathbf{P}(\kappa|j))\mathbf{H}_i'(\kappa) + \mathbf{R}_i(\kappa))^{-1}\nu_i(\kappa)}$$

Then

$$\gamma_{i,j} = \begin{cases} 1 & \text{if } d \leq \beta\,, \\ 0 & \text{otherwise} \end{cases}$$

3) *Update $\hat{\mathbf{x}}(j|j,\kappa)$ using OOSM $\mathbf{y}_i(\kappa)$.*

$$\hat{\mathbf{x}}(j|j,\kappa) = \hat{\mathbf{x}}(j|j) + \gamma_{i,j}\mathbf{W}(j,\kappa)\left[\mathbf{y}(\kappa) - \mathbf{H}(\kappa)\hat{\mathbf{x}}(\kappa|j)\right]$$
$$\mathbf{P}(j|j,\kappa) = \mathbf{P}(j|j) - \gamma_{i,j}\mathbf{W}(j,\kappa)\mathbf{S}(\kappa)\mathbf{W}(j,\kappa)'$$

where

$$\mathbf{W}(j,\kappa) = \mathbf{P}(j,\kappa|j)\mathbf{H}(\kappa)'\mathbf{S}(\kappa)^{-1}$$
$$\mathbf{S}(\kappa) = \mathbf{H}(\kappa)\mathbf{P}(\kappa|j)\mathbf{H}(\kappa)' + \mathbf{R}(\kappa)$$

end for

In order to demonstrate the benefit of the proposed method, Algorithm 1, we generate four types of events related to sensors' status, namely normal, failure, unavailability and change of accuracy. These events are modeled in the same manner as in the simulated scenario (see Section A. While the events are generated off-line, they are completely unknown to the filter both when they occur as well as what the covariance value is. Figures 5 and 6 show an example of the time trace of the events generated for the two scenarios in this section.

1. An Intermittent GPS scenario

In this scenario, the mobile vehicle made use of 8 independent sensors including: two 100Hz MEMS based IMUs, a HMR2300 magnetic compass, an odometer, a barometric altimeter, a Ensco ranging sensor and a TDOA sensor as well as a SPAN GPS. We begin with the case when sensors behavior is nominal, followed

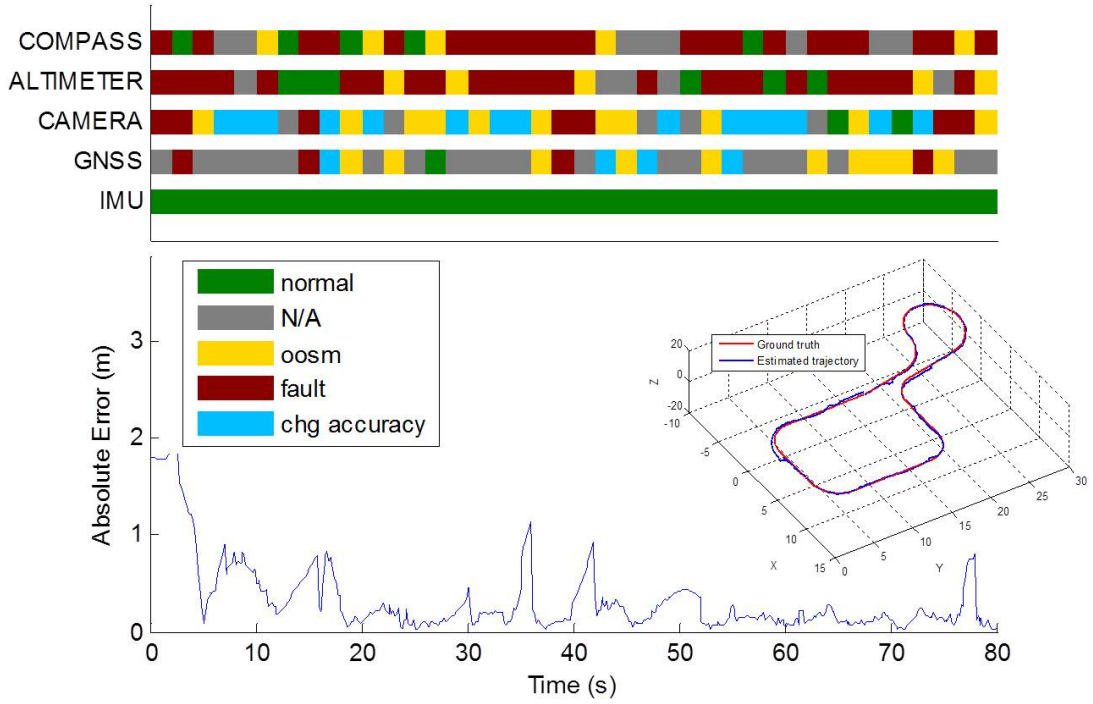

Figure 3. Plot of the RMSE during the filter evolution and the corresponding events in time and comparison of the estimate with the ground truth for simulated scenario.

by randomly generated occurrences of unknown events. The results for the first case are shown in Figure 7. Clearly, using the GPS measurements, the result is particularly good in this case. However, our focus here is not accuracy, but showing that the filter performance can be maintained at a reasonable level despite the presence of multiple unknown events. The simulated events are shown in Figure 5.

Akin to previous subsection, the events are completely unknown to the filter. If the baseline EKF is used in this case (namely the core filter without gating and covariance update), then the estimated trajectory is shown in 8(a). This shows that the EKF goes unstable very quickly even if a GNSS is used. Indeed, after the GNSS becomes unavailable (see Figure 5), as other sensors are experiencing failure/change of accuracy, the EKF is not capable to fuse the measurement in a consistent way, thereby becoming unstable. The subfigures on the top-right of Figure 8(a) indicate that all the sensors are used at all time. Thus, the standard EKF where sensors are more intermittent in their behavior (switching between on/off, failures and change of accuracy), becomes unstable.

Figure 8(b) shows the same EKF as in Figure 8(a) but with the presence of only the gating step (omitting step 2 of Algorithm 1). In this case, the sensor measurements which are incompatible with the underlying model get rejected. As one would expect the results are much better. The time instants at which a sensor gets gated out is shown as a red dot (indicating the value zero for that particular γ) in the top-right subfigures of Figure 8(b). Although the result is better compared to the case when no gating is used (the filter does not diverge), some of the sensors never get used, e.g., the Range sensor (see plots for this sensor always gated).

Figure 8(c) shows the case when the adaptive part (step 3 of Algorithm 1) is active as well. In this case, measurements that get gated out are not just removed from the filtering process but they are used to learn the covariance of the sensor. This leads to results that are much better. Note that in this case the Range sensor gets used, the magnetic compass used at more time instants that the case with only gating. The barometer in this case is gated out more often, compared to before, as the z-axis estimate is in this case better than what the barometer can provide and no other sensor (beside the GNSS) can provide z-axis estimates. Overall, these examples show that the proposed approach can cope with unknown events by graceful degradation of the performance of the filter. If no gating and covariance update is used, a standard

	NORMAL	N/A	OOSM	FAULT	CHG ACCU
IMU	1	0	0	0	0
GNSS	0.1	0.5	0.2	0.1	0.1
CAMERA	0.1	0.1	0.3	0.2	0.3
ALTIMETER	0.1	0.2	0.1	0.6	0
COMPASS	0.1	0.2	0.1	0.6	0

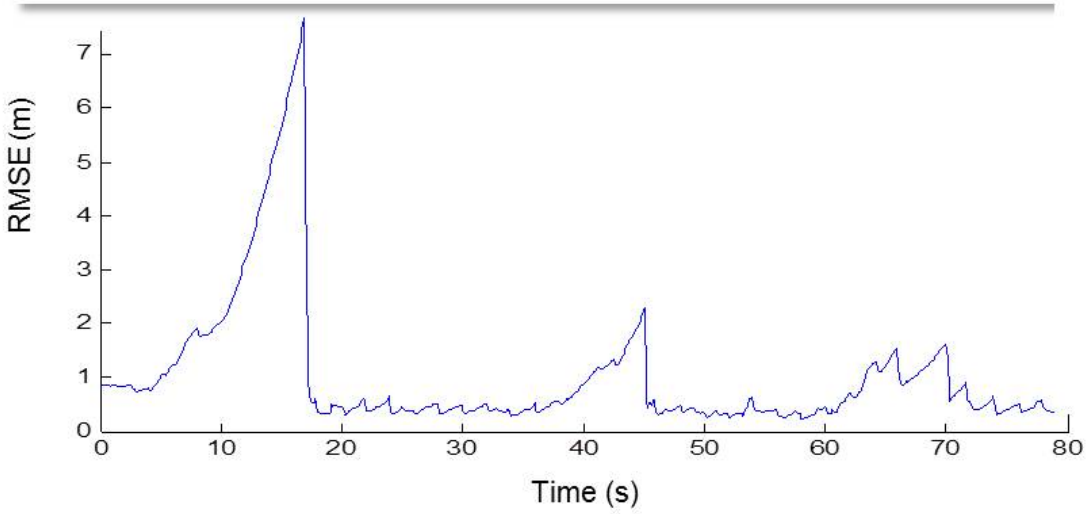

Figure 4. Results on different realizations of events generated via Monte Carlo trials. The probabilities of each event are provided in the table. The RMSE plot is averaged over 50 trials.

EKF goes unstable. Of course, higher accuracy can be obtained by improving the baseline EKF filter (e.g. by using more sensors, etc.). But we re-emphasize that a more accurate EKF would not be robust and adaptive to unknown changes.

2. A GPS Denied scenario

This scenario comprises of the following sensor suite: a 100Hz MEMS based IMU, a HMR2300 magnetic compass, a barometric altimeter, an odometer and a TDOA sensor. This scenario is completely a GPS-denied one. The picture on the left of Figure 9 shows the result of the robust and adaptive EKF used.

Using a baseline EKF filter (with no gating or adaptive covariance learning) on the corrupted data leads to the very poor performance as it is shown in Figure 10(a). Note the large error in the velocity that completely drives the estimate away from the ground truth. In Figure 10(b), we show the filter performance when only gating (omitting step 3 of Algorithm 1) is used. Due to the large number of the events, the filter is not capable of providing a very good estimate.

In Figure 10(c), we report the results when not only the gating is active but the covariance update estimator is also used, namely the results using the proposed approach. In this case, one can clearly see that the estimate is reasonably accurate, follows the ground truth and compares very well with the baseline filter.

For this scenario, we have also considered the effect of OOSMs. Figure 11 shows the generated unknown events, where now, as it can be seen in the figure, some sensors produce measurements with unknown stochastic delays (yellow bar). Using the full estimation framework proposed in this paper, we are able to be robust to the unknown events and OOSMs producing a reasonably good estimate as shown in Figure 12.

We further challenged our solution by making all barometer measurements to be out of sequence and the result is still comparable to that in Figure 12. However, the result without OOSM processing exhibited

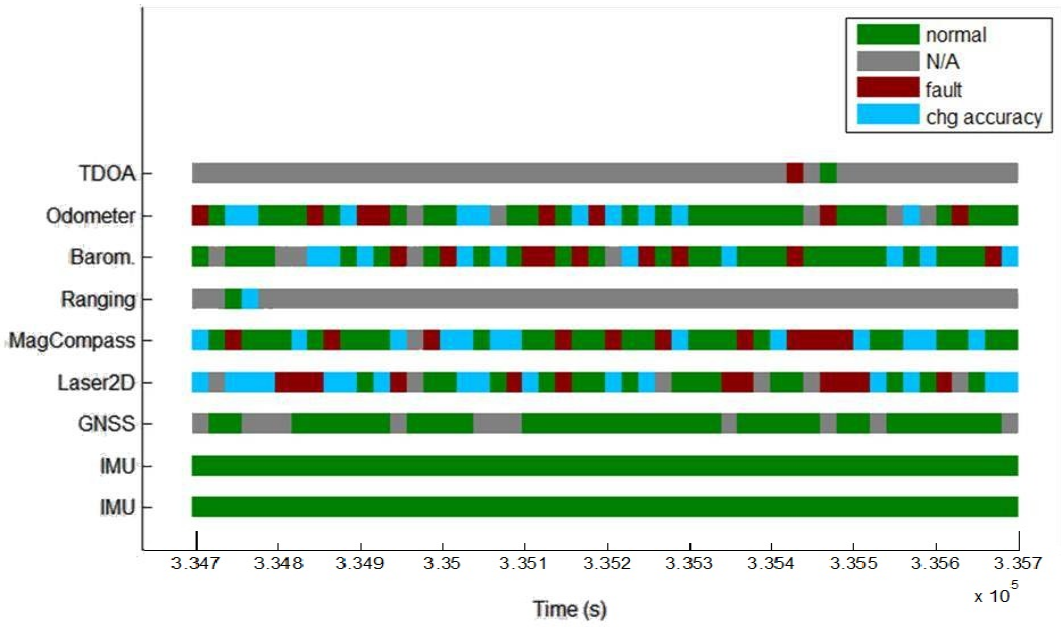

Figure 5. Randomly generated events for the Intermittent GPS Scenario. Time is in GPS weeks, for a total of 15min of data.

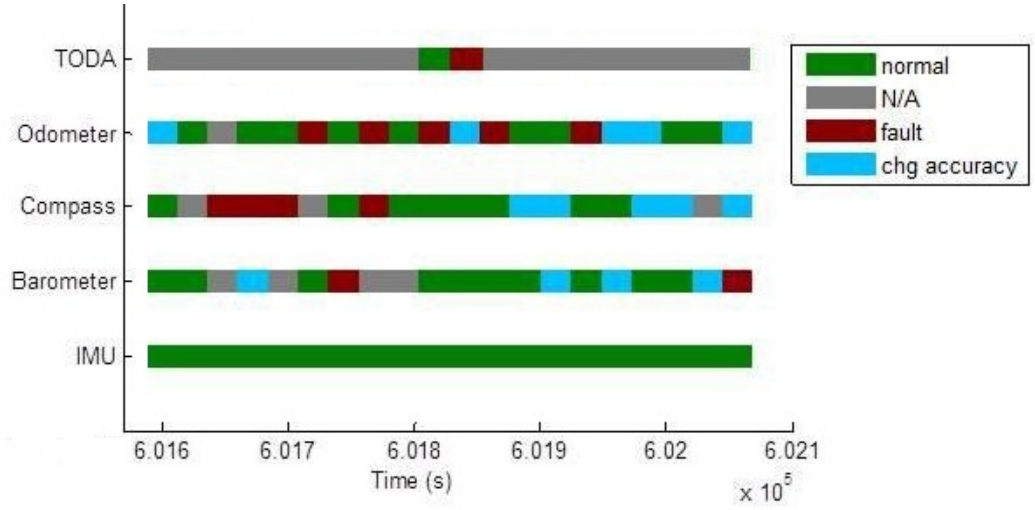

Figure 6. Randomly generated events for the GPS denied scenario. Time is in GPS weeks, for a total of about 5 minutes and 20 seconds of data.

a trend of divergence with maximum error over 1500m. Due to the paper length limit, the result of this scenario is not shown.

In summary, we have demonstrated that in presence of disturbances such as unanticipated changes in sensors' properties and random transmission delays, a standard navigation filter as EKF shows poor performance (possibly instability) compared to the case when sensors operate at nominal models and no OOSMs are present. The use of the proposed approach (Algorithms 1–2) significantly enhanced the navigation robustness in such challenging scenarios and resulted in much less degradation in performance.

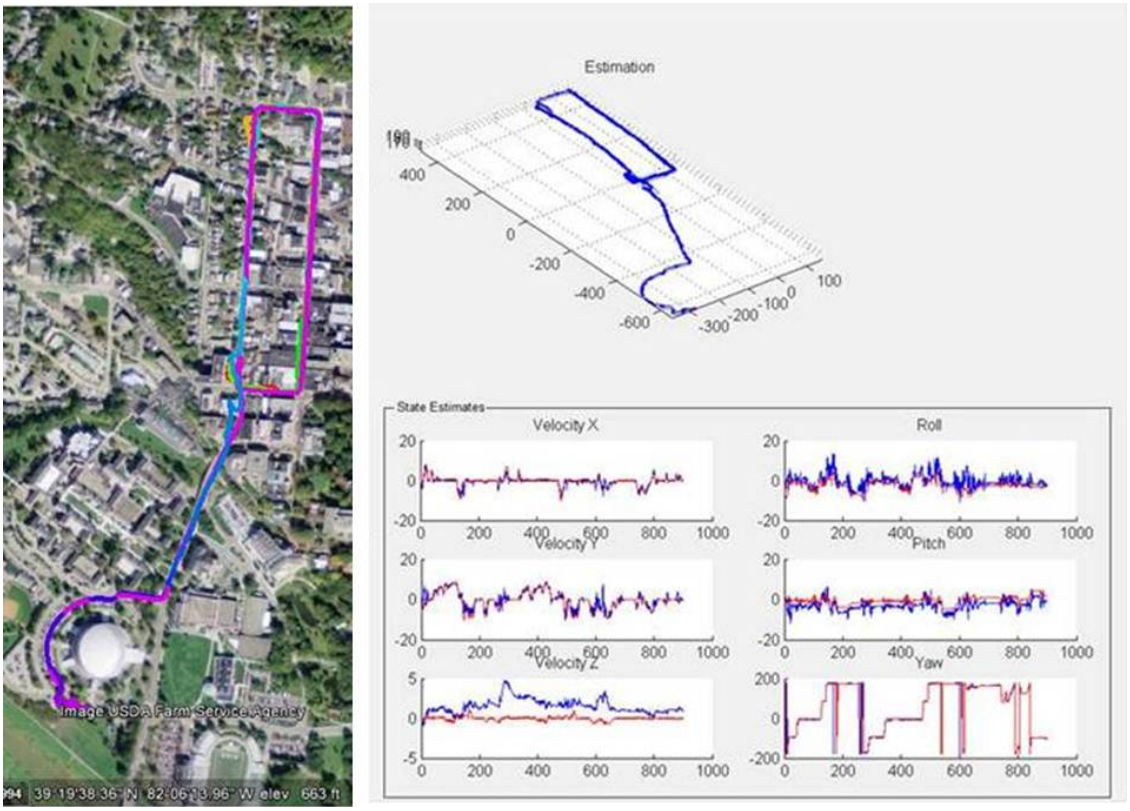

Figure 7. The Intermittent GPS scenario: [Left] Comparison between the ground truth (in pink) and the estimated trajectory. [Right] 3D view of the estimate (blue) and ground truth (gray) as well as the velocity and attitude estimates (blue) and ground truth (red). RMSE is 6m.

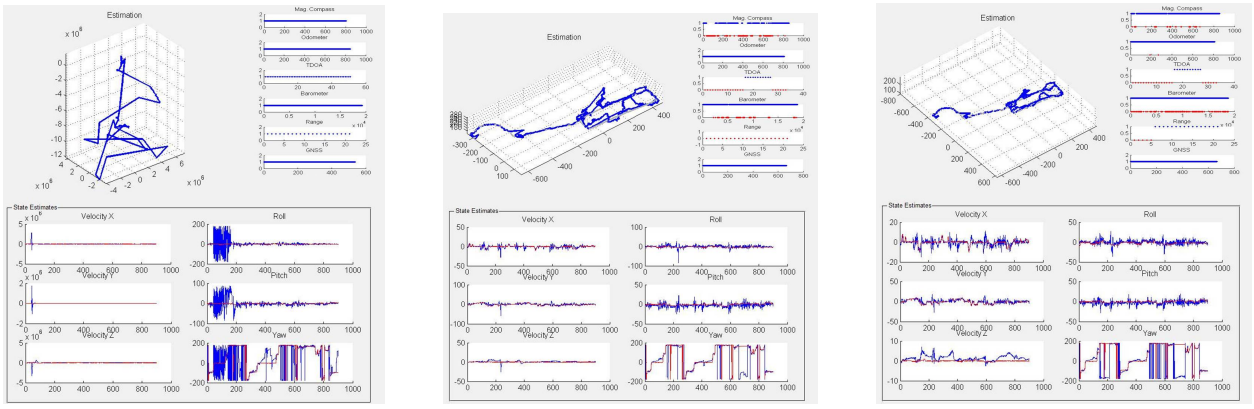

(a) Baseline EKF filter (without gating and covariance update) used on the data corrupted with unknown events.

(b) Robust EKF filter with gating but without covariance update used on the data corrupted with unknown events.

(c) Robust and adaptive EKF filter used on the data corrupted with unknown events.

Figure 8. Intermittent GPS scenario: Estimation results on real data "corrupted" with unknown events using various type of estimators. The small windows on the right of the overall position estimate show the sensor measurements that are used in the filter (blue dots at 1) and that are gated off (red dots at 0). The x-axis represent the measurement number. As it can be noticed the sampling frequencies are different.

IV. Conclusion and Future Work

We presented an estimation framework capable to deal with real world disturbances including outliers, transmission delays and sudden or slow changing of sensor accuracy, as well as numerical issues. The proposed

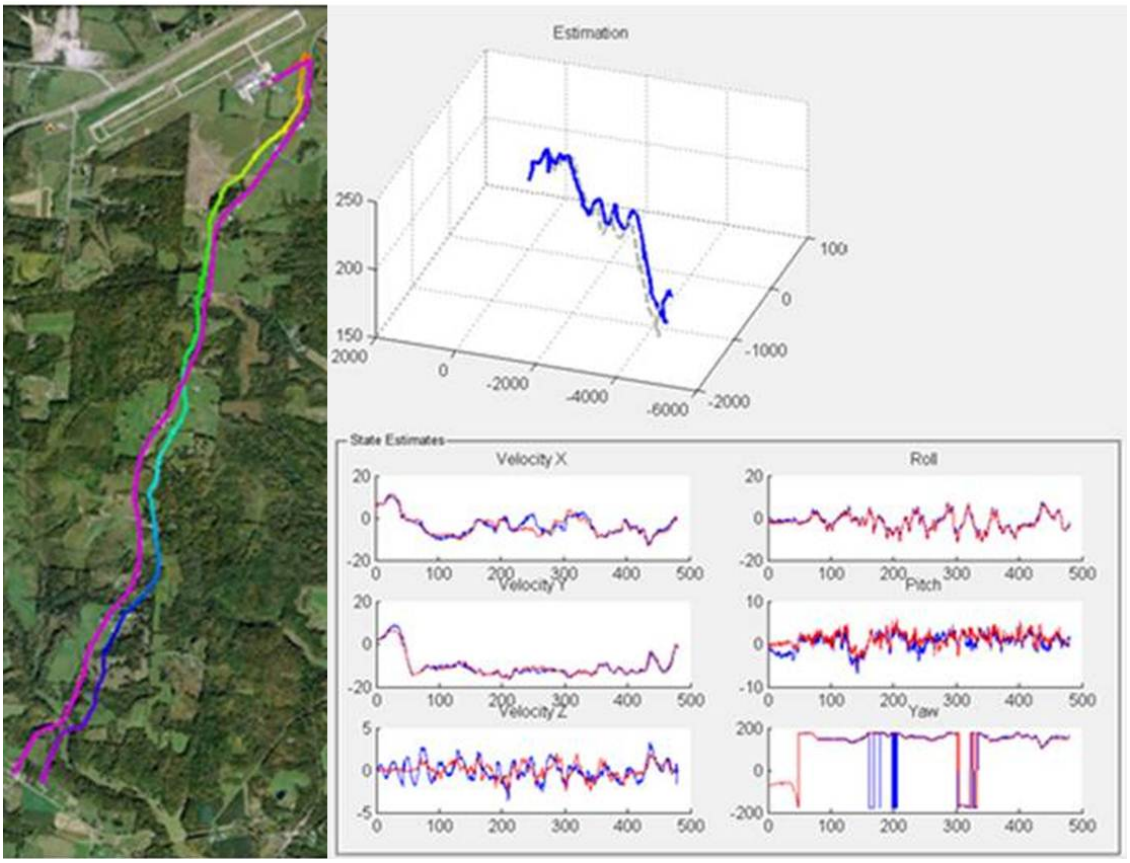

Figure 9. The GPS denied scenario: [Left] Comparison between the ground truth (in pink) and the estimated trajectory. [Right] 3D view of the estimate (blue) and ground truth (gray) as well as the velocity and attitude estimates (blue) and ground truth (red). RMSE is 105m.

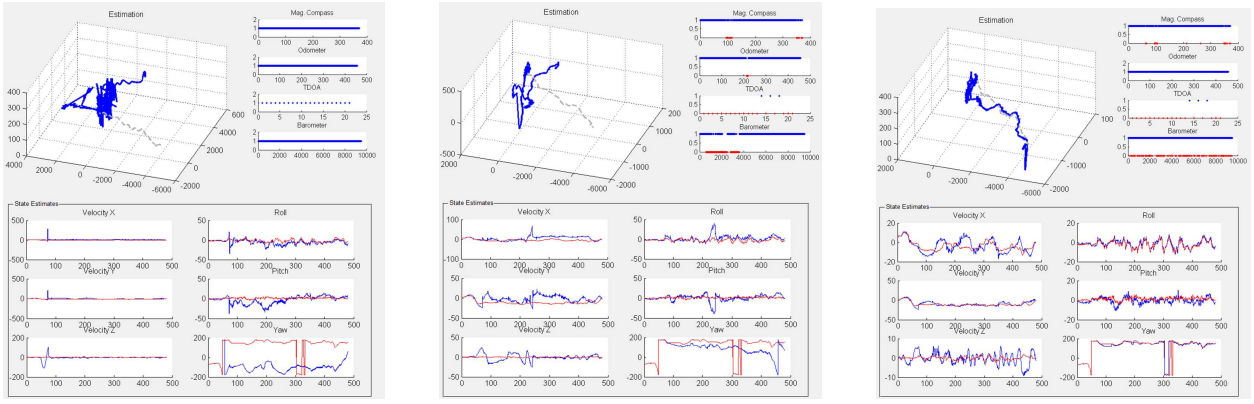

(a) Baseline EKF filter (without gating and covariance update) used on the data corrupted with unknown events.

(b) Robust EKF filter with gating but without covariance update used on the data corrupted with unknown events.

(c) Robust and adaptive EKF filter used on the data corrupted with unknown events.

Figure 10. GPS-denied scenario: Estimation results on real data "corrupted" with unknown events using various type of estimators. The small windows on the right of the overall position estimate show the sensor measurements that are used in the filter (blue dots at 1) and that are gated off (red dots at 0). The x-axis represent the measurement number. As it can be noticed the sampling frequencies are different.

approach features three critical components on top of an existing (legacy), low-complexity filter (e.g. Kalman filter, Extended Kalman Filter), thereby making it much more robust and adaptive in practice. We applied

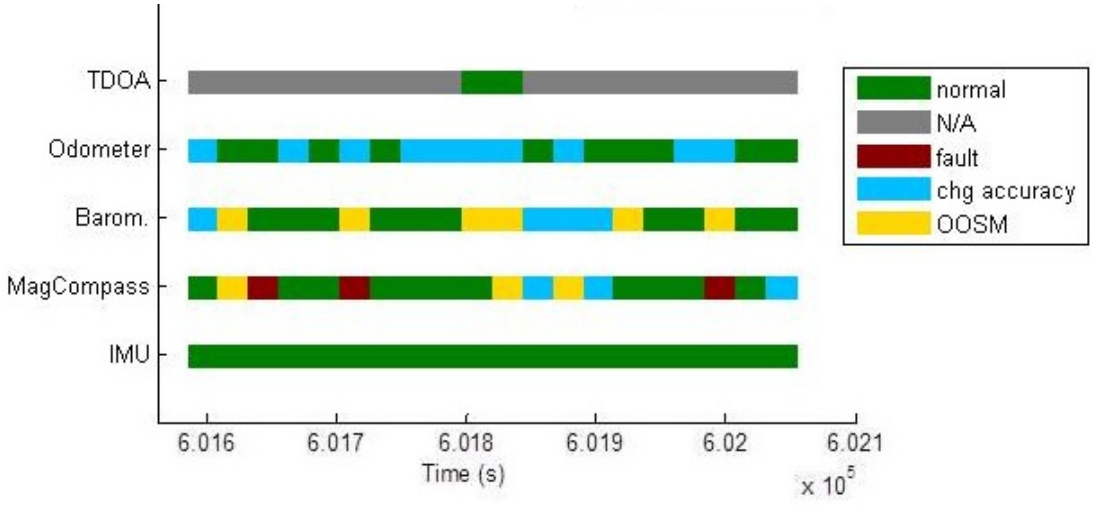

Figure 11. GPS-denied scenario: Randomly generated events including OOSM. Time is in GPS weeks.

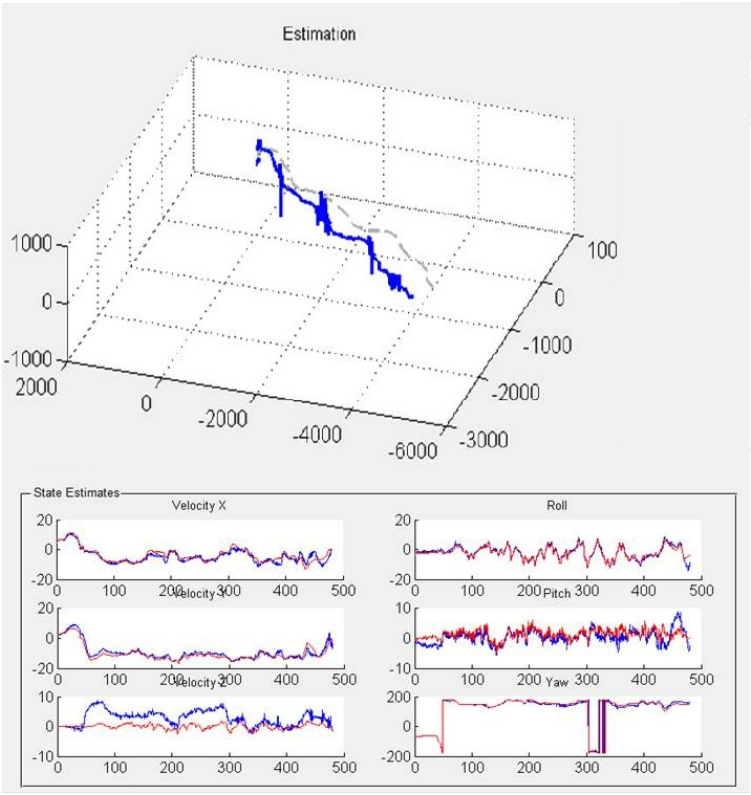

Figure 12. GPS-denied scenario: Robust and adaptive EKF filter used on the data corrupted with unknown events including OOSM.

this approach to simulated as well as real data sets. In all scenarios, we have observed that the navigation robustness was enhanced substantially.

An important future direction we plan to pursue, and for which some preliminary results are available in,[29] is to have a solid theoretical analysis of the proposed framework. Although we have shown it works very well under a large amount of possible events, it is not known under what conditions the filter will be stable and its performance, in terms of, for example, the trace of the error covariance.

A. Proof of Theorem 1

Proof: First, express residue $r(k)$ defined in (4) with respect to the innovation $\nu(k)$

$$\begin{aligned} r(k) &= \mathbf{y}(k) - \mathbf{H}(k)\hat{\mathbf{x}}(k|k) \\ &= \mathbf{y}(k) - \mathbf{H}(k)[\hat{\mathbf{x}}(k|k-1) + \mathbf{K}(k)\nu(k)] \\ &= \underbrace{\mathbf{y}(k) - \mathbf{H}(k)\hat{\mathbf{x}}(k|k-1)}_{\nu(k)} - \mathbf{H}(k)\mathbf{K}(k)\nu(k) \\ &= [I - \mathbf{H}(k)\mathbf{K}(k)]\nu(k) \end{aligned} \tag{6}$$

where $\mathbf{K}(k)$ is the Kalman gain, and hence the covariance of $r(k)$ is given by

$$\begin{aligned} E\{r(k)r(k)'\} &= [I - \mathbf{H}(k)\mathbf{K}(k)]E\{\nu(k)\nu(k)'\}[I - \mathbf{H}(k)\mathbf{K}(k)]' \\ &= [I - \mathbf{H}(k)\mathbf{K}(k)]\mathbf{S}(k)[I - \mathbf{H}(k)\mathbf{K}(k)]' \\ &= \mathbf{S}(k) - \mathbf{H}(k)\mathbf{K}(k)\mathbf{S}(k) - \mathbf{S}(k)\mathbf{K}(k)'\mathbf{H}(k)' + \mathbf{H}(k)\mathbf{K}(k)\mathbf{S}(k)\mathbf{K}(k)'\mathbf{H}(k)' \end{aligned} \tag{7}$$

Substituting $\mathbf{K}(k) = \mathbf{P}(k|k-1)\mathbf{H}(k)'\mathbf{S}(k)^{-1}$ into (7) (except for the last term) yields

$$\begin{aligned} E\{r(k)r(k)'\} &= \mathbf{S}(k) - \mathbf{H}(k)\mathbf{P}(k|k-1)\mathbf{H}(k)' - \mathbf{H}(k)\mathbf{P}(k|k-1)\mathbf{H}(k)' + \mathbf{H}(k)\mathbf{K}(k)\mathbf{S}(k)\mathbf{K}(k)'\mathbf{H}(k)' \\ &= \mathbf{S}(k) - \mathbf{H}(k)\mathbf{P}(k|k-1)\mathbf{H}(k)' - \mathbf{H}(k)[\mathbf{P}(k|k-1) - \mathbf{K}(k)\mathbf{S}(k)\mathbf{K}(k)']\mathbf{H}(k)' \\ &= \mathbf{S}(k) - \mathbf{H}(k)\mathbf{P}(k|k-1)\mathbf{H}(k)' - \mathbf{H}(k)\mathbf{P}(k|k)\mathbf{H}(k)' \end{aligned} \tag{8}$$

Finally, the right hand side (RHS) of (5) can be rewritten by using (8)

$$\begin{aligned} RHS &= E\{r(k)r(k)'\} + \mathbf{H}(k)\mathbf{P}(k|k)\mathbf{H}(k)' \\ &= \mathbf{S}(k) - \mathbf{H}(k)\mathbf{P}(k|k-1)\mathbf{H}(k)' - \mathbf{H}(k)\mathbf{P}(k|k)\mathbf{H}(k)' + \mathbf{H}(k)\mathbf{P}(k|k)\mathbf{H}(k)' \\ &= \mathbf{S}(k) - \mathbf{H}(k)\mathbf{P}(k|k-1)\mathbf{H}(k)' \\ &= \mathbf{R}(k) \\ &= LHS \end{aligned} \tag{9}$$

Q.E.D

References

[1]R. K. Mehra, "On the Identification of Variances and Adaptive Kalman Filtering", in *IEEE Transactions of Automatic Control*, vol. AC-15, no. 2, pp.175–184, April 1970.

[2]F. Gustafsson, *Adaptive Filtering and Change Detection*, Wiley, 2000.

[3]N. Madjarov and L. Mihaylova, "Kalman Filter Sensitivity with respect to Parametric Noises Uncertainty", Kybernetika, Vol. 32 (3), 1996.

[4]F. Busse, and J. How, "Demonstration of Adaptive Extended Kalman Filter for Low Earth Orbit Formation Estimation using CDGPS", in *Institute of Navigation GPS Meeting*, September 2002.

[5]Wang, J., Stewart, M. and Tsakiri, M., "Online Stochastic Modeling for INS/GPS Integration", in *ION GPS-99 proceedings*, 1999.

[6]A. H. Mohamed and K. P. Schwarz, "Adaptive Kalman Filtering for INS/GPS", in *Journal of Geodesy*, vol. 73, pp. 193–203, 1999.

[7]W. Ding, J. Wang, C. Rizos and D. Kinlyside, "Improving Adaptive Kalman Estimation in GPS/INS Integration", in *The Journal of Navigation*, vol. 60, pp. 517–529, 2007.

[8]P. J. Escamilla and N. Mort, A hybrid Kalman filter-fuzzy logic multisensor data fusion architecture with fault tolerant characteristics, in *Proceedings of the 2001 International Conference on Artificial Intelligence (IC-AI2001)*, Las Vegas, Nevada, USA, pp. 361-367, 2001.

[9]D-J. Jwo and H-C. Huang, "GPS Navigation Using Fuzzy Neural Network Aided Adaptive Extended Kalman Filter", in *Proc. of the IEEE Conf. on Dec. and Control and Euro. Cont. Conf.*, Dec. 2005.

[10]C. Hide, T. Moore and M. Smith, "Adaptive Kalman Filtering for Low-cost INS/GPS", in *The Journal of Navigation*, Vol. 56 (1), 2003.

[11]D. Loebis, R. Sutton, J. Chudley and W. Naeem, "Adaptive tuning of a Kalman filter via fuzzy logic for an intelligent AUV navigation system", in *Control Engineering Practice*, Vol. 12, 2004.

[12]B. D. Brumback and M. D. Srinath, "A Chi-square test for Fault Detection in Kalman Filters", in *IEEE Transactions on Automatic Control*, Vol. AC-32, No. 6, June 1987.

[13]Y. Bar-Shalom, X. R. Li, T. Kirubarajan, "Estimation with Applications to Tracking and Navigation", Wiley-Interscience, 2001.

[14]Y. Bar-Shalom, P. Willett and X. Tian, "Tracking and Data Fusion", YBS Publishing, Storrs, CT, 2011.

[15]S-W. Yeom, T. Kirubarajan and Y. Bar-Shalom, "Track Segment Association, FIne-Step IMM and Initialization with Doppler for Improved Track Performance", in *IEEE Transactions on Aerospace and Electronic Systems*, vol. 40, no. 1, pp. 293–309, 2004.

[16]T. Fortmann, Y. Bar-Shalom and M. Scheffe, "Sonar Tracking of multiple targets using joint probabilistic data association", in *IEEE Journal of Oceanic Engineering*, vol. 8 (3), pp. 173–184, Jul 1983.

[17]T. Fortmann, Y. Bar-Shalom, M. Scheffe and S. Gelfand, "Detection thresholds for tracking in clutter–A connection between estimation and signal processing", in *IEEE Trans. Auto. Cont.*, 30 (3), 1985.

[18]W. W. Peterson, T. G. Birdsall, and W. C. Fox, "The theory of signal detectability", in *IRE Trans. on Information Theory*, no. PGIT-4, 1954.

[19]J. Capon, "On the asymptotic efficiency of locally optimal detectors", in *IRE Trans. on Information Theory*, vol. 7 (2), 1961.

[20]Y. Bar-Shalom, "Update with Out-of-Sequence Measurements in Tracking: Exact Solution", *IEEE Trans. Aero. Elec. Sys.*, 38(3), 2002.

[21]M. L. Hernandez et al. "Tracking and Fusion for Wireless Sensor Networks", *Proc. 5th Int. Conf. on Info. Fusion* , 2:1023-1029, 2002.

[22]Z. Jia, A. Balasuriya and S. Challa, "Sensor fusion-based visual target tracking for autonomous vehicles with the out-of-sequence measurements solution", *Rob. and Auto. Systems*, 56:157-176, 2007.

[23]M. Kaess et al., "Concurrent Filtering and Smoothing", *Proc. 15th Int. Conf. on Info. Fusion*, Singapore, Jul. 2012.

[24]S. Zhang and Y. Bar-Shalom, "Optimal update with multiple out-of-sequence measurements with arbitrary arriving order", *IEEE Transactions on Aerospace and Electronic Systems*, IEEE Transactions on Aerospace and Electronic Systems, 48(4):3116-3132, Oct. 2012.

[25]B. Stevens and F. Lewis, *Aircraft Control and Simulation. Wiley*, 1992.

[26]G. Watson, D. H. McCabe and T. Rice, "Multisensor-Multisite Composite Tracking in the Presence of Sensor Residual Bias ", *Proc. SPIE Conf. Sig. Data Proc. of Small Targets*, 1999.

[27]S. Zhang and Y. Bar-Shalom, "Out-Of-Sequence Measurement Processing for Particle Filter: Exact Bayesian Solution," *IEEE Transactions on Aerospace and Electronic Systems* (to appear).

[28]L. E. Dubins., "On curves of minimal length with a constraint on average curvature, and with prescribed initial and terminal positions and tangents", *American Journal of Mathematics*, 79:497-516, 1957.

[29]S. D. Bopardikar, A. Speranzon, S. Zhang and B. Sinopoli, "Performance Analysis of Linear Estimators with Unknown Changes in Sensors Characteristics", Submitted, 2013. Available online at `http://sites.google.com/site/albspe/publications`.